ACS APPLIED MATERIALS & INTERFACES

Research Article

www.acsami.org

Superhydrophobic Surfaces on Light Alloy Substrates Fabricated by a Versatile Process and Their Corrosion Protection

Junfei Ou, Weihua Hu, Mingshan Xue, Fajun Wang,* and Wen Li*

School of Materials Science and Engineering, Nanchang Hangkong University, Nanchang 330063, People's Republic of China

ABSTRACT: After hydrothermally treated in H_2O (for Mg alloy and Al alloy) or H_2O_2 (for Ti alloy), microstructured oxide or hydroxide layers were formed on light alloy substrates, which further served as the active layers to boost the self-assembling of 1H,1H,2H,2H-perfluorooctyltriethoxysilane (PFOTES) and finally endowed the substrates with unique wettability, that is, superhydrophobicity. For convenience, the so-fabricated superhyrdophobic surfaces (SHS) were abridged as HT-SHS. For comparison, SHS coded as CE-SHS were also prepared based on chemical etching in acid and succedent surface passivation with PFOTES. To reveal the corrosion protection of these SHS, potentiodynamic polarization measurements in NaCl solution (3.5 wt %) were performed. Moreover, to reflect the long-term stability of these SHS, SHS samples were immersed into NaCl solution and the surface wettability was monitored. Experimental results indicated that HT-SHS was much more stable and effective in corrosion protection as compared with CE-SHS. The enhancement was most likely due to the hydrothermally generated oxide layer by the following tow aspects: on one hand, oxide layer itself can lower the corrosion due to its barrier effect; on the other hand, stronger interfacial bonding is expected between oxide layer and PFOTES molecules.

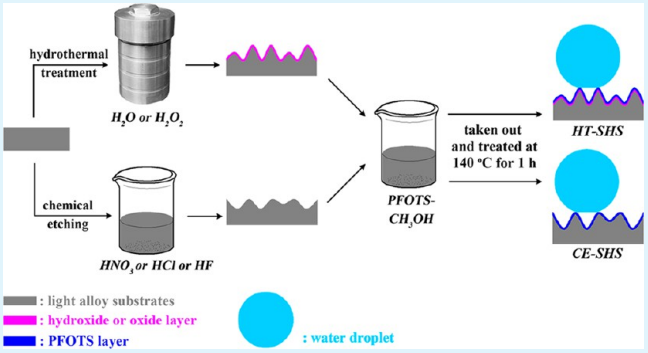

KEYWORDS: *superhydrophobicity, hydrothermal treatment, corrosion protection*

1. INTRODUCTION

Light alloys (i.e., magnesium, aluminum, and titanium alloy) are widely used in aerospace, automobiles, and mechanical apparatus due to their characteristics of low weight, high specific intensity, and good thermal/electrical conductivity.[1−5] However, the inherent poor corrosion resistance has limited their further potential application. Therefore, it is quite necessary to take measures to improve their corrosion resistance.

It is known that the naturally formed oxide layer on light alloy substrate can serve as a corrosion barrier. So, techniques, such as microarc oxidation (MAO), have been developed to generate such passive oxide layer.[6−8] However, the apparatus required by MAO is expensive and the procedure is complicated. Herein, by a simple and versatile hydrothermal process, hydroxide or oxide layers with rough microstructures were prepared on light alloy substrates. The corrosion of the light alloy substrate can be relieved to a certain extent due to the barrier effect of the so-generated oxide layer. To further boost the corrosion protection, the surface was passivated with molecules of 1H,1H,2H,2H-perfluorooctyltriethoxysilane (PFOTES). Correspondingly, the surface energy was lowered and a unique surface wettability, that is, superhydrophobicity, was obtained.

Superhydrophobicity, a special case of wettability with a water static contact angle (SCA) greater than 150° and sliding angle (SA) less than 10°, has aroused considerable interest mainly in two aspects: the fabrication and potential application of superhydrophobic surfaces (SHS).[9,10] As to fabrication, heretofore, many methods including anodization,[11,12] electrodeposition,[13] laser treating,[14] electrospinning,[15,16] chemical vapor deposition,[17] and sol−gel processing[18] have been reported. However, studies about the versatile techniques suitable for a wide range of materials are relatively scarce. A profound example is a simple and versatile chemical etching process to fabricate SHS on a wide range of metal substrates including aluminum, zinc, copper, steel, and titanium alloy.[19,20] Learning from these pioneer research works, it is obvious that such a chemical etching process is suitable for light alloys of aluminum and titanium; however, from the viewpoint of corrosion resistance, SHS obtained by such a chemical etching method is not an ideal choice due to the absence of hydroxide or oxide barrier layer. Thus, it is quite essential to develop another simple and versatile process to prepare SHS with better corrosion protection.[21]

In this paper, a simple and versatile procedure combining the hydrothermal generation of a hydroxide or oxide barrier layer and further passivated with low-surface-energy molecules has been proposed to fabricate SHS on light alloy substrates. The procedure is very impressive for its universality, novelty, and

Received: January 2, 2013
Accepted: March 15, 2013
Published: March 15, 2013

   dx.doi.org/10.1021/am4000134 | ACS Appl. Mater. Interfaces 2013, 5, 3101−3107

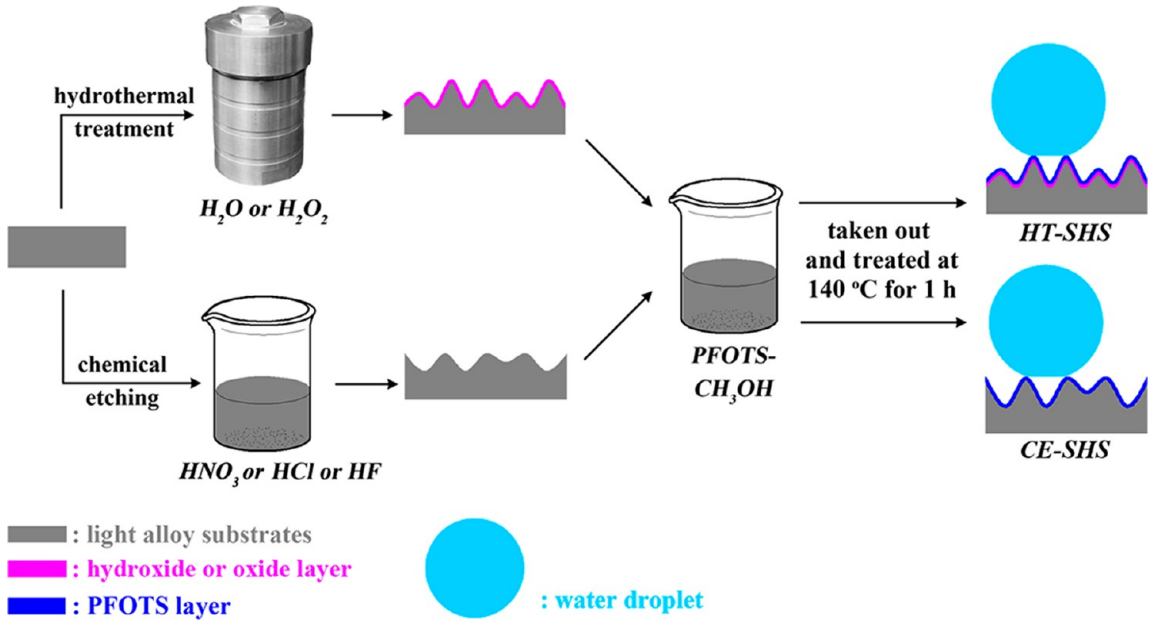

Figure 1. Schematic illustration for the preparation process of SHS on light alloy substrates based on hydrothermal or chemical etching treatments.

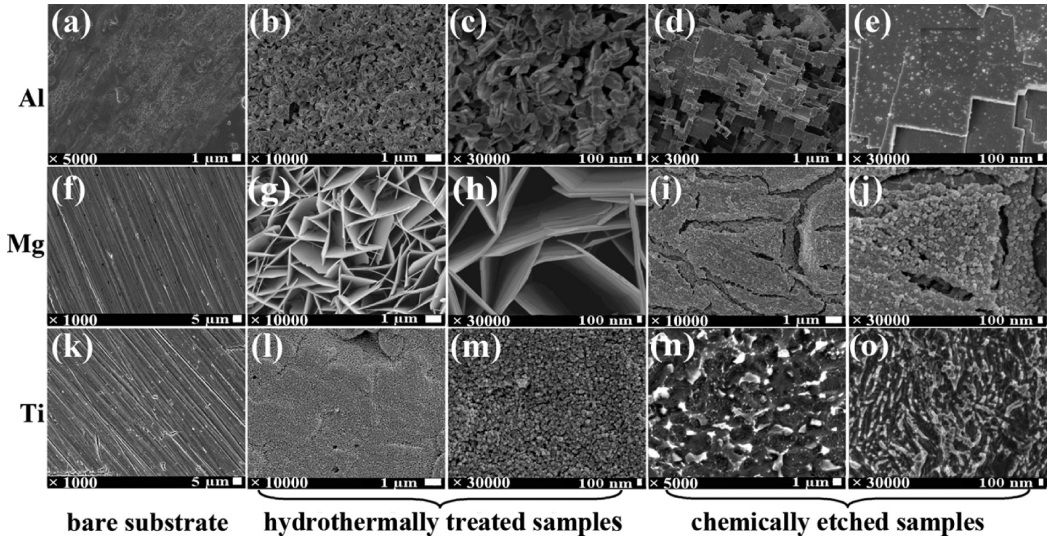

Figure 2. FESEM images of different samples.

simplicity; moreover, the chemical used for hydrothermal treatment is H_2O or dilute H_2O_2, which has no or low impact on environment. The outstanding corrosion protection of the so-obtained SHS has also been confirmed by electrochemical corrosion tests. So, it is hoped that this facile technique will accelerate the production of SHS on light alloys with corrosion resistance applications.

2. EXPERIMENTAL SECTION

2.1. Materials and Reagents. Mg alloy (AZ91D), Al alloy (5083), Ti alloy and (TC4) were obtained from Northwest Institute of Nonferrous Metal Company, China. 1H,1H,2H,2H-perfluorooctyltriethoxysilane (PFOTES) was purchased from Sigma-Aldrich. Other reagents are analytical grade and used as received. Ultrapure water with a resistivity great than 18.0 MΩ·cm was used.

2.2. Preparation of SHS. A schematic view is depicted in Figure 1 to illustrate the fabrication process of SHS on light alloy substrates. First, to get rid of surface contamination, the samples were ground with abrasive paper (600 Cw and 1200 Cw) and ultrasonicated in acetone, ethanol, as well as ultrapure water for 10 min each. Then, the alloy substrates were introduced into a Teflon vessel with a 100 mL capacity. For Mg alloy and Al alloy samples, the vessel was filled with ultrapure water; for Ti alloy, the vessel was filled with H_2O_2 (10%) solution. The vessel was sealed with a lid and maintained at a temperature of 120 °C for 6 h. After this, the samples were taken out and cleaned in ultrapure water for 5 min and dried with N_2 gas. Then, the samples were immersed in a methanol solution (1.0 wt %) of PFOTES at room temperature for 1 h followed by heat treatment at 140 °C for 1 h. Finally, the samples were ultrasonically cleaned in acetone and ethanol. For convenience, the so-fabricated superhyrdophobic surfaces (SHS) were abridged as HT-SHS.

Control SHS abridged as CE-SHS were also prepared by a similar process by replacing the hydrothermal treatment with chemical etching process. The details of chemical etching are as follows: the Al/Mg/Ti alloy substrates were immersed into HCl (3.7 wt %), HNO_3 (6.8 wt %), and HF (4.0 wt %) solution, respectively, for 5 min at ambient temperature.

2.3. Characterizations. An optical contact angle meter (Easydrop, Krüss, Germany) with a computer-controlled liquid dispensing system

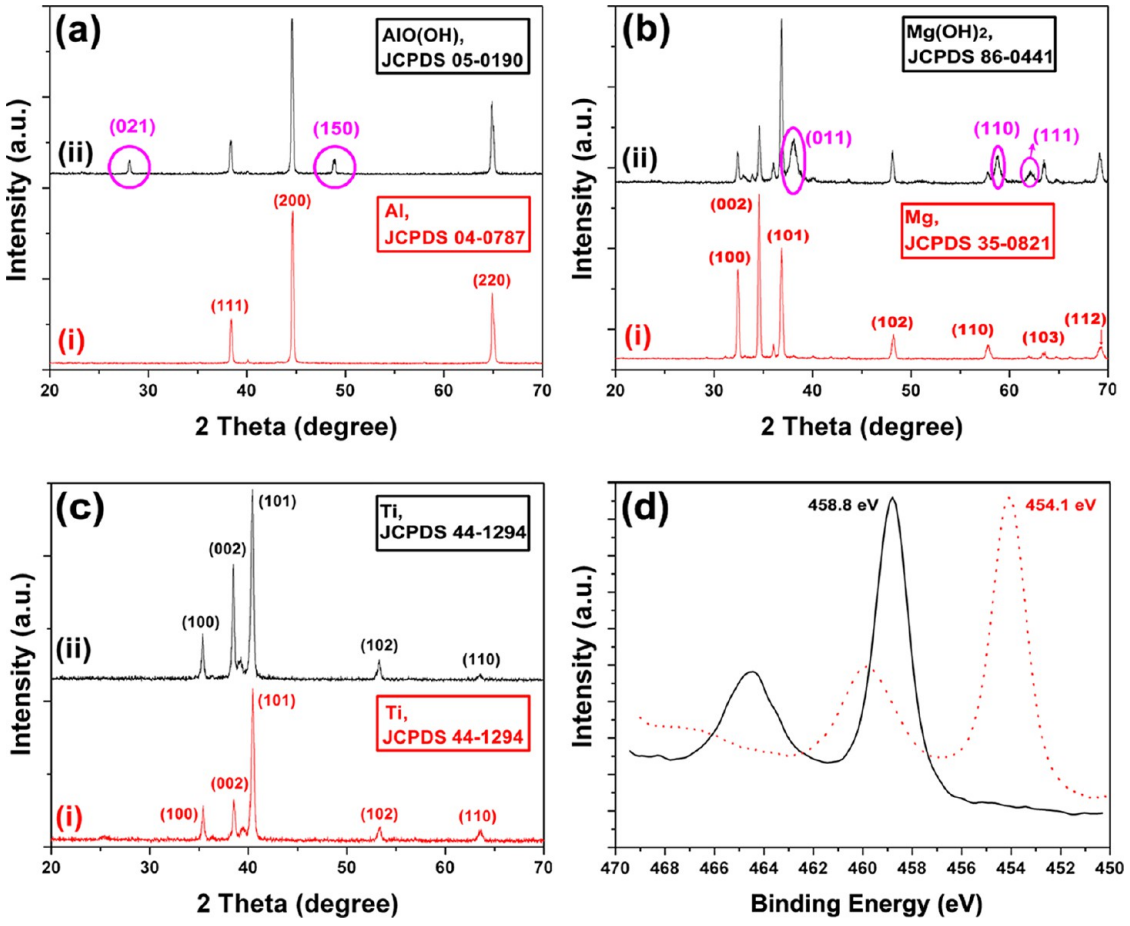

Figure 3. XRD patterns of the chemically etched (i) and hydrothermally treated (ii) samples (a–c). (d) Ti 2p XPS of the chemically etched (dashed line) and hydrothermally treated (solid line) Ti alloys.

and a motorized tilting stage was used to measure water static contact angle (SCA) and sliding angle (SA) at ambient temperature (24 °C). A voume of 7 μL of ultrapure water was dropped onto the samples, and the SCAs were determined by different positions (>5) of the same samples. To estimate the long-term durability of superhydrophobic properties under continuous contact with seawater, the samples were soaked in NaCl (wt. 3.5%) solution for a long time. After a definite time of immersion, the sample was taken off the water, dried under a nitrogen stream, and retained in a vacuum oven at 30 °C for 60 min.[22−24] Then, the wettability of the samples was measured by the method mentioned above.

The morphological microstructures were observed on a field emission scanning electron microscope (FE-SEM, JEOL, JSM-6701F, Japan) under vacuum environment, and the samples were presputtered with a thin palladium/gold film. The chemical compositions of the samples were studied by X-ray photoelectron spectroscopy (XPS, Physical Electronics, PHI-5702). The measurements were performed using a monochromated Al Kα irradiation and the chamber pressure was about 3×10^{-8} Torr under testing condition. The binding energy of adventitious carbon (C1s: 284.8 eV) was used as a basic reference.

Electrochemical corrosion test was performed on an electrochemistry workstation (CS350, Wuhan Corrtest Instrument Co., Ltd., China) by potentiodynamic polarization in a three-electrode system: a working electrode (WE), a platinum stick counter electrode, and a saturated calomel reference electrode (SCE). NaCl solution of 3.5 wt % was used as the electrolyte. Dynamic measurement of polarization curves in a Tafel model was acquired at a scan rate of 1 mV/s at room temperature.

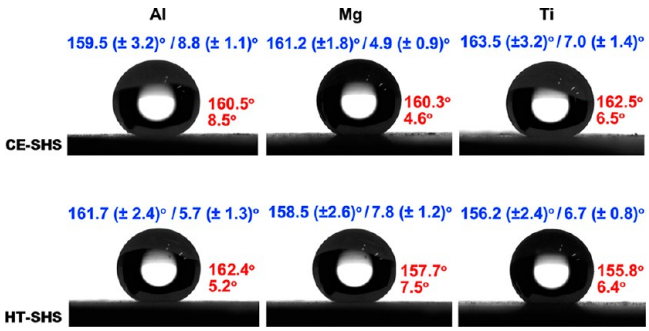

Figure 4. SCA images for water droplets on SHS and related data. SCA/SA value of the depicted image is marked beside the droplet with red and the average data of each sample is marked above the droplet in blue.

3. RESULTS AND DISCUSSION

3.1. Surface Topographies and Species. To characterize the surface features of various samples, FESEM images are provided in Figure 2. For bare substrates, abrasive grooves are observed [Figure 2 (a), (f), and (k)]. After hydrothermal treatment, for Al (Figure 2b, c) and Mg alloy (Figure 2g, h) substrates, the surfaces are composed of petal-shaped nanosheets with a typical thickness of ∼100 nm; moreover, the "petals" on Al alloy surface seem to be smaller and packed more closely. For hydrothermally treated Ti alloy substrate (Figure 2l, m), the surface is composed of nanoparticles with diameter

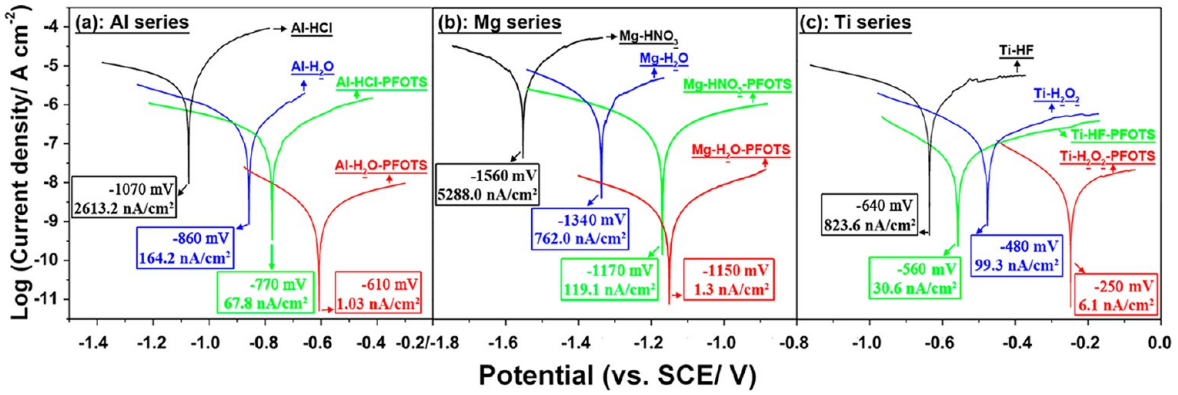

Figure 5. Tafel plots of different samples. Corrosion potential (E_{corr}) and corrosion current density (I_{corr}) derived from the curves were denoted in the rectangles.

of ~100 nm. The surface topographies of the chemically etched samples are quite different as compared with the hydrothermally treated ones. Figure 2d and e shows that the fractal morphology in 3-D is formed with numerous facets that form a large number of cavities deep in the chemically etched Al alloy substrate surface, just as reported by Wu et al., and Qian et al.[11,19] For Mg alloy substrate (Figure 2i, j), cracks with wideness ranging from ~200 nm to ~1 μm are formed; moreover, it is observed that the surface is covered by nanoparticles with a typical diameter of ~100 nm (Figure 2j). For Ti alloy substrate (Figure 2n), microstructures with cavities as well as islands are distributed uniformly across the surface. Under larger magnification (Figure 2o), it is clearly observed that the surface of cavities or islands is covered with nanopapillae with a typical scale of several tens of nanometers. The formation of such surface microstructures on the etched samples is because that the alloy is made of different elements (such as Ti, Al, V for TC4 Ti alloy; Mg, Al, Zn for AZ91D Mg alloy; Al, Mg for 5083 Al alloy), the etching rate at different positions of the surface is unequal.[20] The special topographies of the hydrothermally treated samples are originated from the newly formed surface species, such as hydroxide and oxide, due to the reactivity of Al/Mg/Ti with water or H_2O_2.

To discover the surface species, XRD patterns of different samples were given in Figure 3. It is apparent that the chemically etched samples show strong signals of the major composition of light alloys (Figure 3a, Al; Figure 3b, Mg; Figure 3c, Ti]. While, for the hydrothermally treated samples of Al and Mg alloys, some new peaks attributed to hydroxide [AlO(OH) or $Mg(OH)_2$] appear. It is supposed that such species are generated by the reaction equations of eqs 1 and 2.

$$Mg + 2H_2O = Mg(OH)_2 + H_2 \quad (1)$$

$$2Al + 4H_2O = 2AlO(OH) + 3H_2 \quad (2)$$

$$Ti + 2H_2O_2 = TiO_2 + 2H_2O \quad (3)$$

However, for Ti alloy, there is no new peak. This may result from the following two aspects: no species are formed by hydrothermal treatment or the formed species are amorphous and cannot be detected by XRD. To get further information, XPS of Ti alloys treated by chemical etching or hydrothermal is also provided. It is observed that the Ti $2p_{3/2}$ for chemical etching sample is located 454.1 eV, which is a typical value of Ti(0) metal.[25,26] For hydrothermally treated samples, Ti $2p_{3/2}$ shifts to a higher binding energy of 458.8 eV, implying that the Ti atoms are positively charged. Moreover, this value is very similar to the reported ones of TiO_2.[27−29] So, it is deduced that a layer of TiO_2 has been generated under the oxidation of H_2O_2 (eq 3).

3.2. Wettability. The surface wettability is evaluated by an optical contact angle meter. It is observed that, for the grinding and degreasing treated bare substrates, SCAs are dispersed in wide ranges (Al, 11°~22°; Mg, 10°~20°; Ti, 10°~25°). Such wide dispersions may be partly due to the grooved surface structures (Figure 2a, f, and k), which are expected to break the axial symmetry of the water droplet and finally result in the phenomenon that SCA will depend on drop orientation with respect to image plane. After CE or HT treatment, grooved structures disappeared and such orientation-SCA dependence is alleviated. Correspondingly, the SCA dispersion range becomes narrower (HT-Al, <10°; HT-Mg, <10°; HT-Ti, <10°; CE-Al, 10°~16°; CE-Mg, <10°; CE-Ti, 15°~25°). The low SCA of the chemically etched samples is probably due to the high activity of the freshly prepared alloy surfaces and capillarity of the special microstructures. For the hydrothermally treated samples, the superhydrophilicity is mainly supposed to be related not only with the microstructures but also the generated hydrophilic hydroxide [$Mg(OH)_2$, AlO(OH)] or oxide (TiO_2) layer.

After modified with PFOTES, SCA increases sharply: for bare substrates (Al, Mg, and Ti alloy) modified with PFOTES, SCAs increase to 112.5° (±2.6°), 115.4° (±3.2°), and 114.8° (±2.8°), respectively; for HT and CE treated samples, SCAs are greater than 150° and SA less than 10° (as shown in Figure 4), suggesting that SHS are obtained. The origin of this special wettability, that is, superhydrophobicity, is generally believed to be related with two important parameters of low surface energy and rough surface microstructures. Herein, the former parameter is realized by surface passivation with low-surface-energy molecules of PFOTES; the latter one is realized by HT or CE treatment (as seeing from Figure 2, rough microstructures are formed after HT or CE treatment).

3.3. Corrosion Protection. In order to estimate the corrosion protection of the generated hydroxide or oxide layer and SHS, Tafel plots were measured (Figure 5) when stable open circuit potential (OCP) was obtained after the samples being exposed to NaCl solution for a certain period. Important parameters, such as corrosion potential (E_{corr}) and corrosion current density (I_{corr}) can be derived from the curves. It is generally believed that lower I_{corr} value denotes lower corrosion dynamic rate and positive E_{corr} represents lower corrosion

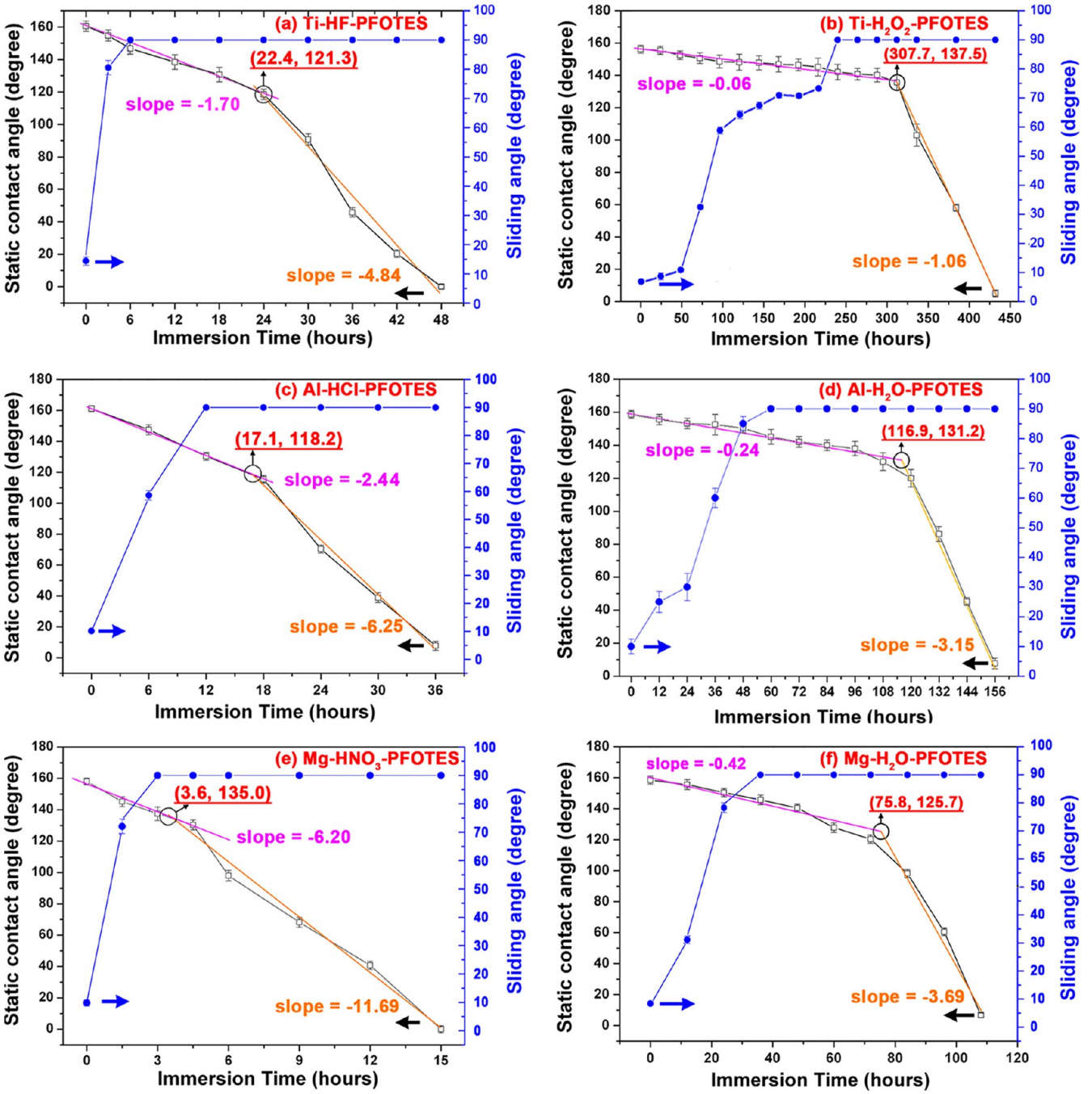

Figure 6. Surface wettability variation as a function of immersion time.

thermodynamical tendency. The highest I_{corr} and most negative E_{corr} of black plots in Figure 5 suggests that the chemically etched light alloy substrates are easiest to be corroded. This is mainly because that, after being chemically etched, fresh and active surface is obtained and the corrosion chemical reactions are easy to occur. For the hydrothermally treated samples, protective layers [such as AlO(OH), Mg(OH), and TiO_2] are formed, so the I_{corr} decreases and E_{corr} shift positively, as shown in Figure 5. After modified with low-surface-energy molecules of PFOTES, SHS is obtained and the corrosion protection is enhanced greatly. Moreover, SHS based on hydrothermal treatment is more effective in corrosion protection, this is mainly because that the generated hydroxide or oxide layer can serve as a barrier layer to obstruct the diffusion of water and other corrosive species (such as Cl^- and O_2) dissolved in water.

The above-mentioned corrosion behaviors were based on a short-term immersion process (about 30 min). To further characterize the long-term stability of SHS under the attack of corrosive species (such as water, oxygen, and chloride ions), the so-fabricated SHS were immersed into NaCl solution for a much longer period (tens to hundreds of hours) and the surface wettability, including SCA and SA, of these samples was measured (Figure 6). It is obvious that SCA decreases gradually from >150° to about 10° and SA increases from <10° to 90°. This wettability variation suggests that the low-surface-energy molecules on SHS are deteriorated as the immersion time prolonging. Moreover, it is observed that the deterioration rate,

dx.doi.org/10.1021/am4000134 | ACS Appl. Mater. Interfaces 2013, 5, 3101−3107

which can be reflected by the slope of the fitted lines in Figure 6, was much lower for SHS-HT as compared with SHS-CE. This is probably because that the interfacial interaction between the substrate and PFOTES molecules is quite different for the samples of SHS-HT and SHS-CE. Specifically, for SHS-HT, reactive substrate surfaces with hydroxyl groups were generated and PFOTES molecules were expected to be self-assembled thereon;[26,30,31] therefore, there may exist covalent interfacial bonding of ≡Si—O—Me (Me denotes metal substrate of light alloy, ≡Si is the silicon atom on the hydrolyzed PFOTES molecules). For SHS-CE, by a chemical etching process, there generate no functional surface groups which can react with PFOTES or its hydrolysates; so, weak interfacial interaction such as physical adsorption is expected. In the literature,[32,33] the wettability evolution and mechanism analysis of various SHS on substrates has been discussed in detail. It is concluded that there are two common reasons for the deterioration of SHS under continuous contact with water. On one hand, at the SHS/liquid interface, the hydrophobic molecules are exposed to liquid directly; under the attack of water or other components, some hydrophobic molecules tend to desorbed from the substrate through certain reactions, such as hydrolysis of chemical interfacial bonding ≡Si—O—Me

$$\equiv Si—O—Me + H_2O \Rightarrow \equiv Si—OH + Me—OH$$

On the other hand, it is detected that water molecules can be adsorbed at the SHS/vapor interface. Under the above situations, water molecules are confirmed to penetrate the SHS to reach the substrate. This may also trigger the desorption of hydrophobic molecules. From these discussions, it can be seen that the deterioration of superhydrophobicity is greatly governed by the desorption of hydrophobic molecules, which is much difficult to occur for chemisorbed ones. So, it can be well understood that the SHS with chemical interfacial bonding[34,35] can endure much longer immersion period as compared with ones with weak physical adsorption.

It is also observed that there exists a kink in the SCA–immersion time curve. Before the kink, SCA decreases slowly; after it, SCA decreases more rapidly. This might be because that, at the earlier stage, PFOTES molecules are packed closely and the corrosion is suppressed. However, under the persistent attack of corrosive species, PFOTES layers will finally be deteriorated and some defects (such as micro- or nanoholes) formed, which conversely facilitate more severe corrosion and result in faster deterioration.

4. CONCLUSIONS

Two kinds of SHS (i.e., CE-SHS and HT-SHS) were fabricated on light alloy substrates and their corrosion protection was investigated. Experimental results indicate that HT-SHS is a much better choice for corrosion protection due to the following two aspects: on one hand, the so-generated hydroxide or oxide can serve as a barrier la,yer to obstruct the diffusion of water and other corrosive species (such as Cl^- and O_2) dissolved in water; on the other hand, the so-generated hydroxide or oxide layer is expected to be abundant with active surface hydroxyl groups, which may further induce the chemical anchoring of perfluoroalkylsilane and finally impart SHS with much better tolerance to corrosion medium such as NaCl solution. In one word, HT-SHS is an ideal candidate for corrosion protection for its simple preparation process, low or no impact on environment, and effectiveness.

AUTHOR INFORMATION

Corresponding Author

*Tel.: +86-791-6453210. Fax: +86-791-6453210. E-mail: wenl@ualberta.ca (W.L.); jjbxsjz@yahoo.cn (F.W.).

Notes

The authors declare no competing financial interest.

ACKNOWLEDGMENTS

The authors acknowledge with pleasure the financial support of this work by the National Natural Science Foundation of China (Grant Nos. 21203089 and 51263018), International S&T Cooperation Program of China (Grant No. 2012DFA51200), and Jiangxi Provincial Department of Education (Grant No. GJJ12422).

REFERENCES

(1) Lutjering, G.; Williams, J. C. *Titanium*, 2nd ed.; Springer: 2007.
(2) Fu, Y.; Song, Y.; Hui, S.; Mi, X. *Chin. J. Rare Met.* **2006**, *30*, 850 (in Chinese).
(3) Gurrappa, I. *Mater. Charact.* **2003**, *51*, 131.
(4) Kaufman, J. *Introduction to aluminum alloys and tempers*; ASM International: 2011; pp 87–118.
(5) Easton, M.; Beer, A.; Barnett, M.; Davies, C.; Dunlop, G.; Durandet, Y.; Blacket, S.; Hilditch, T.; Beggs, P. *JOM* **2008**, *60*, 57.
(6) Liu, P.; Pan, X.; Yang, W.; Cai, K.; Chen, Y. *Mater. Lett.* **2012**, *75*, 118.
(7) Wang, H.; Liu, F.; Zhang, Y.; Yu, D.; Wang, F. *Appl. Surf. Sci.* **2011**, *257*, 5576.
(8) Rao, K. P.; Ram, G. D. J.; Stucker, B. E. *Scr. Mater.* **2008**, *58*, 998.
(9) Zhang, Y.; Chen, Y.; Shi, L.; Li, J.; Guo, Z. *J. Mater. Chem.* **2012**, *22*, 799.
(10) Fan, X.; Jiang, L. *Adv. Mater.* **2008**, *20*, 2842.
(11) Wu, W.; Wang, X.; Wang, D.; Chen, M.; Zhou, F.; Liu, W.; Xue, Q. *Chem. Commun.* **2009**, 1043.
(12) Wang, D.; Hu, T.; Hu, L.; Yu, B.; Xia, Y.; Zhou, F.; Liu, W. *Adv. Funct. Mater.* **2009**, *19*, 1930.
(13) Zhao, N.; Shi, F.; Wang, Z.; Zhang, X. *Langmuir* **2005**, *21*, 4713.
(14) Jin, M.; Feng, X.; Xi, J.; Zhai, J.; Cho, K.; Feng, L.; Jiang, L. *Macromol. Rapid Commun.* **2005**, *26*, 1805.
(15) Ma, M.; Hill, R.; Lowery, J.; Fridrikh, S.; Rutledge, G. *Langmuir* **2005**, *21*, 5549.
(16) Ma, M.; Mao, Y.; Gupt, M.; Gleason, K.; Rutledge, G. M. *Macromolecules* **2005**, *38*, 9742.
(17) Hozunu, A.; Takai, O. *Thin Solid Films* **1997**, *303*, 222.
(18) Tadanaga, K.; Morinaga, J.; Matsuda, A.; Minami, T. *Chem. Mater.* **2000**, *12*, 590.
(19) Qian, B.; Shen, Z. *Langmuir* **2005**, *21*, 9007.
(20) Qu, M.; Zhang, B.; Song, S.; Chen, L.; Zhang, J.; Cao, X. *Adv. Funct. Mater.* **2007**, *17*, 593.
(21) Gupta, N.; Sasikala, S.; Barshilia, H. C. *Nanosci. Nanotechnol. Lett.* **2012**, *4*, 757.
(22) Boinovich, L. B; Emelyanenko, A. M.; Pashinin, A. S. *ACS Appl. Mater. Interfaces* **2010**, *2*, 1754.
(23) Boinovich, L. B.; Emelyanenko, A. M.; Pashinin, A. S.; Lee, C. H.; Drelich, J.; Yap, Y. K. *Langmuir* **2012**, *28*, 1206.
(24) Ivanova, N. A.; Philipchenko, A. B. *Appl. Surf. Sci.* **2012**, *263*, 783.
(25) Moulder, J.; Stickle, W. F.; Sobol, P. E.; Bomben, K. D. *Handbook of X-ray Photoelectron Spectroscopy*, 2nd ed.; Perkin Elemer Corporation: Eden Prairie, MN, 1992.
(26) Ou, J.; Liu, M.; Li, W.; Wang, F.; Xue, M.; Li, C. *Appl. Surf. Sci.* **2012**, *258*, 4724.
(27) Ou, J.; Wang, J.; Zhang, D.; Liu, S.; Yan, P.; Liu, B.; Yang, S. *Colloids Surf., B Biointerfaces* **2010**, *76*, 123.
(28) Collins, R. J.; Shin, H.; DeGuire, M. R.; Heuer, A. H.; Sukenik, C. N. *Appl. Phys. Lett.* **1996**, *69*, 860.

(29) Zhang, F.; Jin, S.; Mao, Y.; Zheng, Z.; Chen, Y.; Liu, X. *Thin Solid Films* **1997**, *310*, 29.
(30) Ishizaki, T.; Sakamoto, M. *Langmuir* **2011**, *27*, 2375.
(31) Ou, J.; Wang, J.; Zhou, J.; Liu, S.; Yu, Y.; Pang, X.; Yang, S. *Prog. Org. Coat.* **2010**, *68*, 244.
(32) Boinovich, L. B.; Emelyanenko, A. M. *Adv. Colloid Interface Sci.* **2012**, *179*−*182*, 133.
(33) Boinovich, L. B.; Gnedenkov, S. V.; Alpysbaeva, D. A.; Egorkin, V. S.; Emelyanenko, A. M.; Sinebryukhov, S. L.; Zaretskaya, A. K. *Corros. Sci.* **2012**, *55*, 238.
(34) Wasserman, S. R.; Tao, Y. T.; Whitesides, G. M. *Langmuir* **1989**, *5*, 1074.
(35) Fontaine, P.; Goldmann, M.; Rondelez, F. *Langmuir* **1999**, *15*, 1348.